

RESEARCH

Open Access



# A wearable low profile asymmetrical slotted ultra-wide band antenna for WBAN applications

S. Jayakumar\* and G. Mohanbabu

\*Correspondence:  
sjayakumarece@gmail.com

Department of ECE, SSM Institute  
of Engineering and Technology,  
Dindigul, Tamil Nadu, India

## Abstract

In this article a low profile asymmetrical slotted Ultra-Wide Band (UWB) antenna is proposed for Wireless Body Area Networks (WBANs) applications. The antenna was fabricated using Printed Circuit Boards (PCBs). An improved radiation pattern was obtained with an optimized patch shape of the antenna that broadens the bandwidth and lowers the antenna's profile. The proposed antenna is simulated in HFSS and CST Simulator, and the proposed antenna is fabricated on FR4 substrate with the reduced ground plane. In frequency ranges from 2.50 to 10.97 GHz simulation as well as measured results show that the reflection coefficient ( $S_{11}$ ) of the antenna is below  $-10$  dB and increased impedance bandwidth of 126%. The proposed antenna has desired radiation pattern and gain for wearable application. The wearable performance of proposed antenna on chest, leg, and the arms of the human body is analyzed with Specific Absorption Rate (SAR). The maximum value of the SAR is 0.785 W/Kg which is less than threshold value of 1.6 W/kg. The time-domain behavior of proposed antenna is investigated with the time domain parameters such as Group delay, Fidelity factor and Mean realized gain. The time domain results are evident for the proposed antenna is capable of pulse signal transmission and reception.

**Keywords:** Low profile, UWB antenna, WBAN, Specific Absorption Rate (SAR)

## 1 Introduction and motivation

WBAN is a rapidly growing technology that fascinated many researchers owing to its real-time applications in health care monitoring, army, and sports, etc.

The prerequisite of user-friendly, Cost-effective low power multifunctional WBAN systems is directed to develop UWB Technology. The WBAN system needed an antenna to transmit the signals from the WBAN to medical devices for real-time monitoring of the patient. The Ultra-wideband antenna (UWB) has unlicensed bandwidth coverage of 3.1–10.6 GHz that is allowed by the FCC [2].

UWB technology has a high data rate across a short communication range [1], Compactness, minimal mutual coupling between the human membrane and the antenna with low backward radiation, tailored time and frequency characteristics, higher radiation efficiency with wide bandwidth, and good impedance matching are essential requirements for WBAN system applications.

An antenna on the human body plays an essential role in the operation of the WBAN system. Wearable position on the humane body and movements of user will cause polarization mismatch and the absorption loss is major challenge to design an antenna for wearable application. However, antenna design should take into account the antenna's impact on the human body. So the UWB antenna having vertical polarization is desirable for the WBAN system. Initially, Microstrip Patch Antennas were presented, but they only partially met the above requirements, hence several strategies to improve antenna performance were introduced [3–5].

Patches on UWB antennas come in a variety of shapes, including rectangular, circular, square, elliptical, and triangular. Slotted ground systems are recommended to enhance bandwidth while minimizing the influence of the ground plane [6, 7]. A reduced ground plane is another commonly used strategy for improving bandwidth in UWB antenna [8]. Textile antennas [9] are easily sewn on the cloth; however, it is more sensitive to moisture content. Full ground plane textile antennas are vulnerable to deformation. The geometry of a flexible UWB antenna [10] that has a full ground plane is complex, and the bandwidth of a monopole antenna with a microstrip feed could not cover the full UWB range of frequencies.

The shape of antenna is analyzed by calculating the entropy [11–13] of the antenna. Slotted ground plane is used [14] to broaden the bandwidth multiband operation. A novel Discrete Shapelet Transform is used [15] for time frequency-shape analysis. The fractal antennas are provided multiband operation with wide bandwidth [16].

The proposed UWB antenna should be built with compactness to address the problems in the above literature. So in this article, Low Profile Asymmetrical Slotted UWB Antenna is Proposed, fabricated, and tested for problem specifications. The proposed UWB antenna has a physical dimension of 17.5 mm × 30.0 mm and covers a frequency range from 2.5 to 10.97 GHz which is suitable for WBAN applications.

In Sect. 2 the proposed antenna is carefully designed for wearable application. In Sect. 3, the time domain behavior and frequency domain behavior of the proposed antenna are analyzed with simulation and measured results, and the wearable performance is also discussed. In Sect. 4 is conclusion.

## 2 Antenna structure and design

The unique design of UWB antennas with the same outer dimension is depicted in Fig. 1a–d. An elliptical patch is depicted in Fig. 1a and it is covered partial bandwidth over the UWB range. Strip is added diagonally to make antenna asymmetry structure and the radiation performance has been improved comparing to elliptical radiator then slot has been introduced for the better performance. Slots has been included by random scheme and parametric study is helpful to optimize the patch dimension of the antenna.

To choose a suitable antenna, the four antennas are simulated and compared. The reflection co-efficient ( $S_{11}$ ) of four antennas are compared and the results are shown in Fig. 1e. The results show that the proposed design is desirable for WBAN applications.

The proposed UWB antenna has a slotted elliptical-shaped asymmetrical slotted patch with the ground plane. Figure 2 depicts dimensions of the proposed UWB antenna. It is designed on FR4 substrate which has a thickness of 1.6 mm, and a Slotted elliptical-shaped patch and Microstrip feed line having a length ( $l_f$ ) of 8.3 mm and width ( $W_f$ ) of

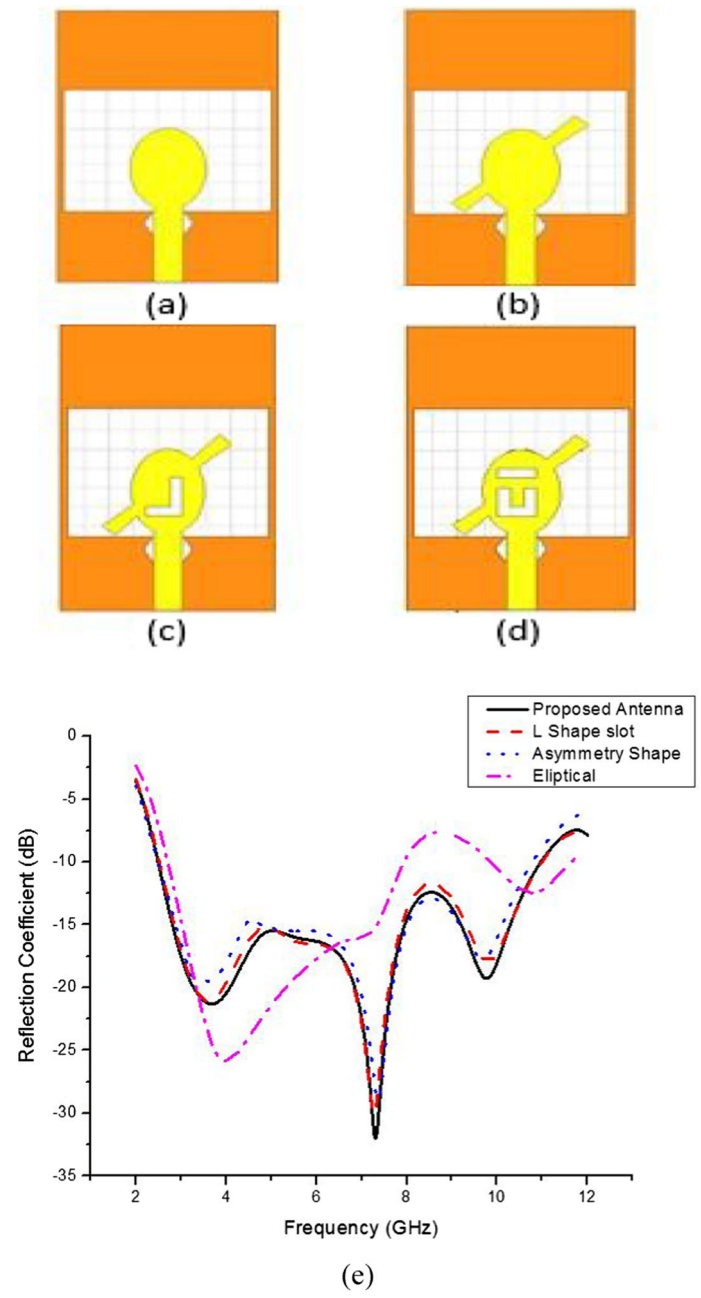


**Fig. 1** a–d UWB antennas with same outer dimensions and **e** Reflection coefficient comparison of (a–d)

2.3 mm is printed on the same surface of the FR4. The opposite side of FR4 is partially grounded with a hexagonal slot under the feed line. The optimized dimensions are

$$W = 17.5 \text{ mm}, L = 30 \text{ mm}, w_p = 5.76 \text{ mm}, l_p = 9 \text{ mm}, l_{g1} = l_{g2} = 8.25 \text{ mm},$$

$$l_{gs} = 13.5 \text{ mm}, W_{gs1} = 7 \text{ mm}, W_{gs2} = 4.5 \text{ mm}, l_{fs} = 1.54 \text{ mm}$$

This antenna design operates in the range of frequency between 2.5 and 10.97 GHz which produces the reflection coefficients of  $-23 \text{ dB}$ ,  $-33 \text{ dB}$ , and  $-20 \text{ dB}$ , respectively,

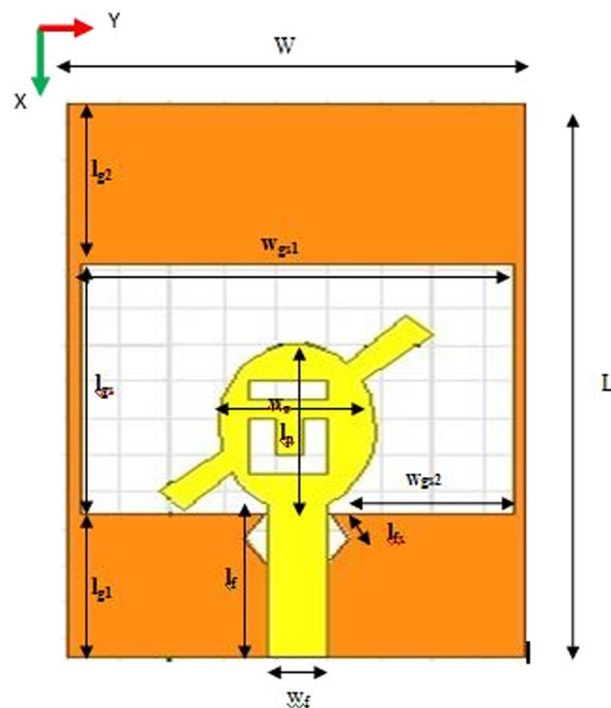


**Fig. 2** Proposed UWB antenna dimensions

at 3.6 GHz, 7.4 GHz, and 9.8 GHz frequencies. The length of the Ground Plane plays a vital part in wideband antenna design. At low frequencies, the current is more concentrated to achieve proper impedance matching.

At symmetrical conditions current supplied by the feed line is distributed uniformly on the surface of the patch. When adding a strip diagonally the antenna is become an asymmetrical, so the distribution of current is uneven over the patch because of the unbalanced current distribution, maximum radiation occurred at higher frequencies and the antenna's impedance bandwidth is enhanced.

The slot in ground plane is specifically observed to play a significant role to increase the antenna bandwidth which is due to electromagnetic interaction in the slotted ground plane. The asymmetric patch design with offset feed plays a major role in maintaining proper impedance matching. As an effect of coupling between the asymmetrical radiating patch and slotted ground, the lower and higher limit of resonance frequency is expanded. So the antenna's impedance bandwidth is improved.

### 3 Results and discussion

The proposed UWB antenna is simulated by HFSS simulator, and results are validated by using CST Simulator. In this section, behavior of the antenna in both the time and frequency domains was examined.

#### 3.1 Frequency—domain behavior

The antenna performance in the frequency domain is analyzed in this section. The Simulation and Measured results of  $S_{11}$ , radiation characteristics and VSWR are

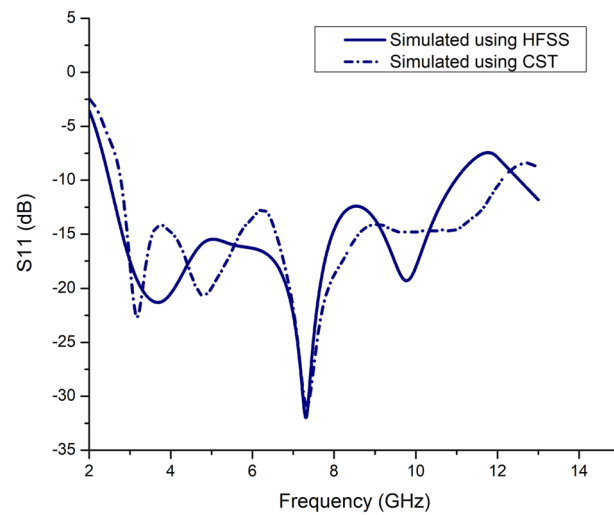


**Fig. 3** Simulation result of proposed antenna in HFSS and CST

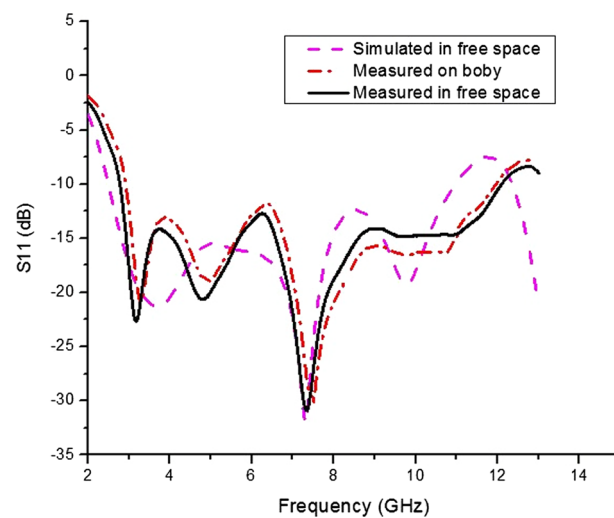


**Fig. 4** Comparison of simulated  $S_{11}$  with measured  $S_{11}$  on the body and free space

discussed. To investigate the human body effect fabricated antenna is tested on the surface of the human body and also in free space.

The  $S_{11}$  of proposed antenna simulated by Finite Element Method (FEM) based HFSS. In order to validate  $S_{11}$  of the antenna, the same design was simulated using CST simulator. The simulation result using the FEM solver reported a bandwidth of 2.5 to 10.97 GHz, whereas the impedance bandwidth by the finite difference transient solution ranged from 2.5 to 12 GHz which is shown in Fig. 3.

The MS2037C VNA Master is utilized to take measurements of the antenna. The results of the antenna were plotted using Origin pro. The antenna is resonated at 3.6 GHz, 7.4 GHz, and 9.8 GHz and spanned an impedance bandwidth of 2.50 GHz to 10.97 GHz during the measurement process which is shown in Fig. 4. Almost all the

results were uniform in the UWB frequency range and there was a small variation at some frequency. The small variation was caused by the antenna fabrication process.

Another reason could be substrate losses. The patch of the proposed antenna was asymmetric and had a slotted defective ground plane leads to reduce the antenna's size and the electric field distribution changed as the current flow was reduced. So that the bandwidth of the antenna is enhanced and impedance matching of antenna also improved.

Measurements of  $S_{11}$  on the body and free space are shown in Fig. 4. The results proved that the impact of the suggested design on the human body has a negligible effect. Moreover, the Measured results are slightly different from simulated results.

The radiation performance of the proposed design is analyzed by HFSS and CST tools. The far-field radiation pattern is measured in an anechoic chamber at 3.6 GHz, 7.4 GHz and 9.8 GHz. The simulated results and measured results in  $xoy$ -plane and  $yozy$ -plane at various frequencies are depicted in Fig. 5.

The proposed antenna radiates Omni-directionally in the  $xoy$  plane ( $E$  Plane). The radiation pattern has some variation at high frequencies due to higher-order mode resonance. The proposed antenna's radiation performance is suitable for WBAN over the full UWB band.

VSWR value is a numerical indicator, and it is helpful to understand the status of impedance matching to which it is connected. A perfectly matched antenna has VSWR value of one. Figure 6 shows the VSWR Variation through the entire UWB Band. VSWR variations are acceptable over the UWB range.

### 3.2 Time domain behavior

The performance of the antenna in time domain is also essential to analyze. The behavior of antenna in the time domain can be understood with time domain parameters of Fidelity Factor, Group delay and Mean Realized Gain (Figs. 7, 8, 9, 10).

Mean Realized Gain (MRG) is an indicator to understand the radiation characteristics of the proposed UWB antenna in the UWB range. The MRG can be formulated as

$$\text{MRG}(r) = \frac{1}{\text{BW}_n} \int_{f_i}^{f_h} G_r(r, f) df$$

Group delay demonstrates time distortion behavior between two antennas. Two UWB antennas are set to face to face with a far-field distance of 120 mm. Figure 8 shows the group delay of the proposed antenna. It is flat over the UWB range of frequencies with less variation of 0.3 ns. Within UWB band the signal transmission is good without any distortion.

Figure 9 depicts simulated and measured MRG over the UWB range of frequency from 2.5 to 10.97 GHz. MRG was obtained from 3 to 5 dBi across UWB Band to understand the correlation between broadcast and received signals the fidelity factor of the antenna is helpful. It calculates the signal distortion induced by a two-antenna setup. The Fidelity Factor of Proposed antenna is depicted in Fig. 10 The fidelity factor indicates excellent time-domain behavior at different azimuthal angles.

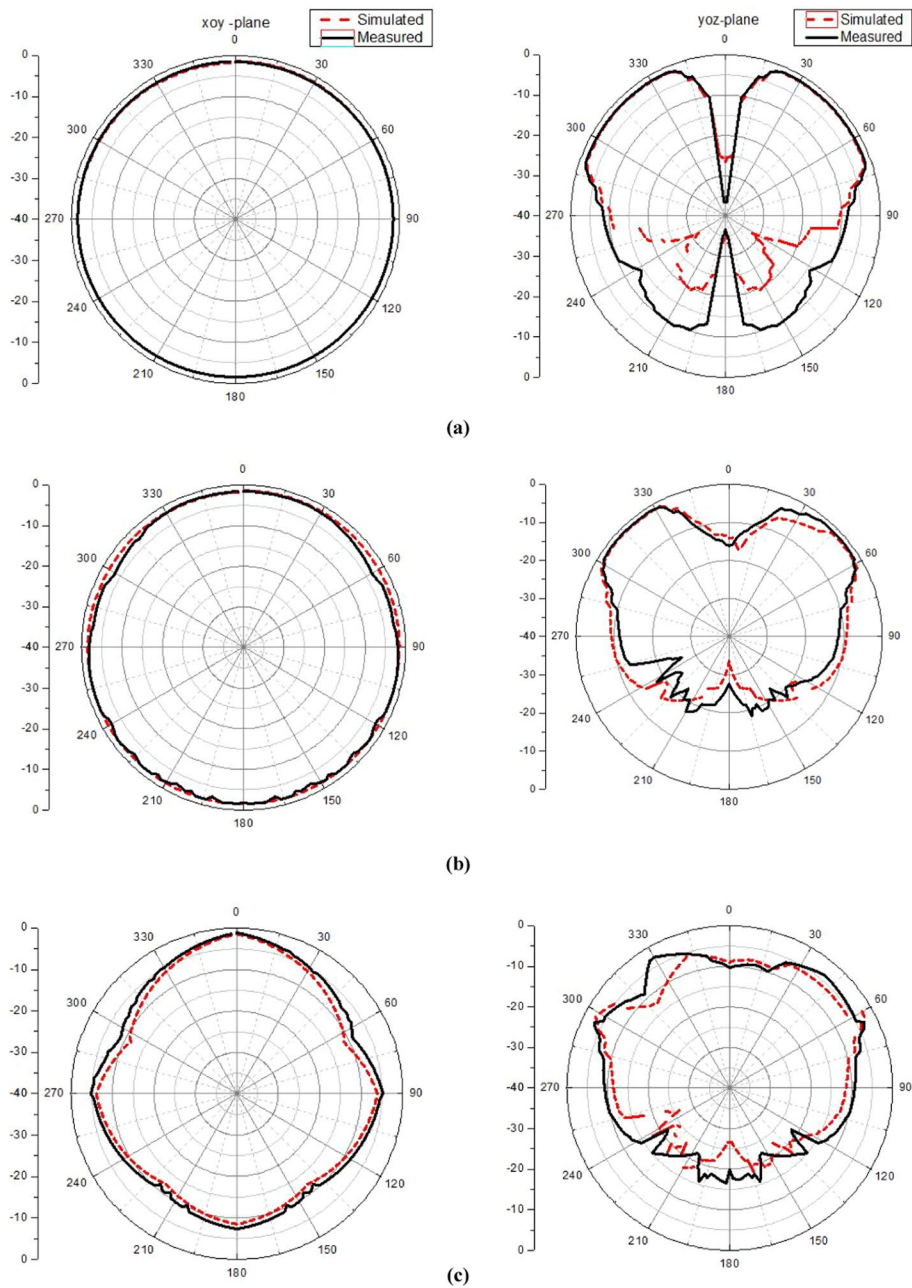


**Fig. 5** Radiation pattern **a** 3.6 GHz, **b** 7.4 GHz, **c** 9.8 GHz

Table 1 shows the Comparison of the Proposed Antenna with the Existing design. It shows that the Proposed design has an improved bandwidth with a compact size.

### 3.3 Wearable performance and SAR analysis

Wearable performance of the proposed antenna is analyzed by placing the antenna in various parts of humane body [11]. The  $S_{11}$  is measured when antenna placed on chest, leg, and the arms. The measured results compared with free space measurement that shows that the effect of humane body is negligible. The proposed antenna covered the

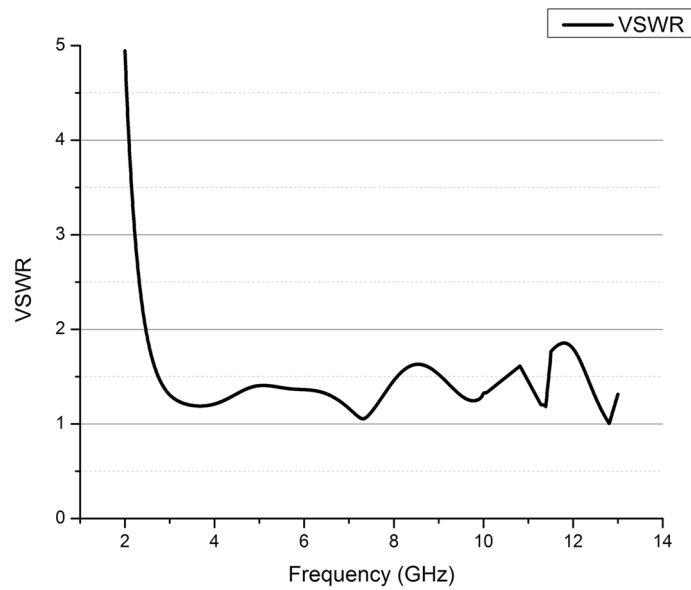


**Fig. 6** VSWR variation over UWB range

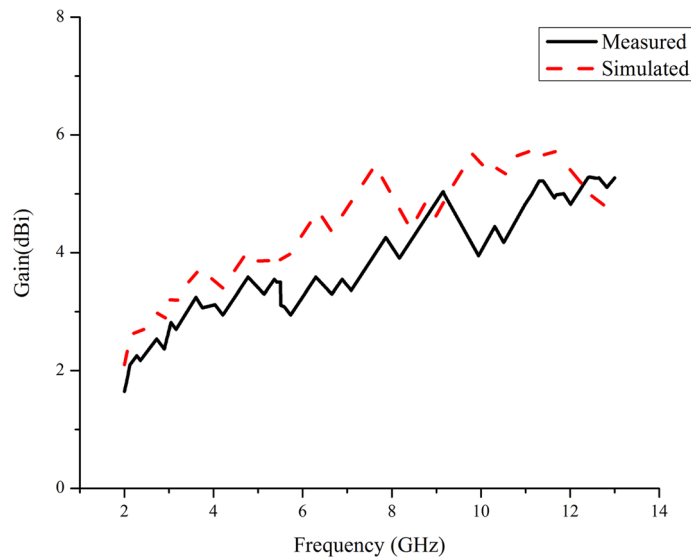


**Fig. 7** Simulated and measured gain over UWB frequency

entire UWB band of frequency irrespective of position of antenna. However it is essential to analysis the Specific Absorption Rate (SAR) value.

Rate at which energy is absorbed by the human body when exposed to RF radiation is called Specific Absorption Rate. Either the American standard or the European standard can be used to study the effects of radiation on the human body. The FCC regulation stipulates that the SAR threshold value is 1.6 W/kg averaged over 1 g of humane tissue. The International Electro-technical Commission (IEC), which enforces European standards, established a threshold value for SAR of 2 W/kg averaged across 10 g of humane



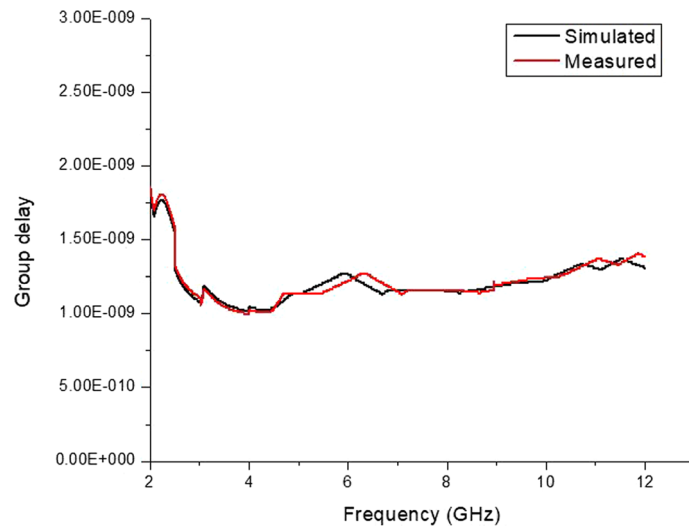


**Fig. 8** Group delay of the proposed antenna

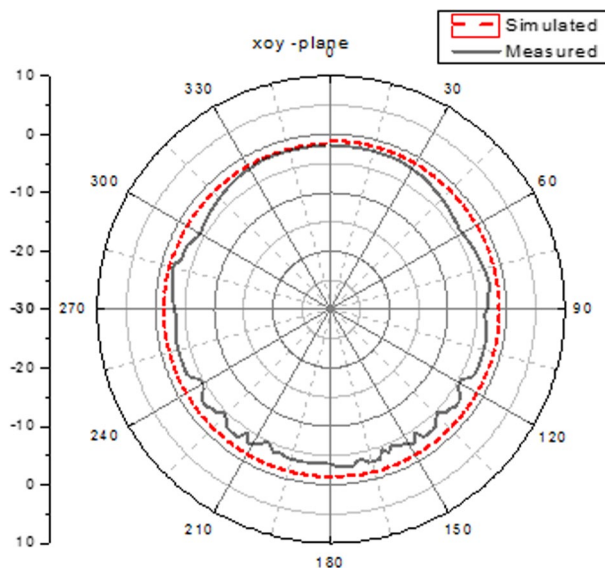


**Fig. 9** Simulated MRG and measured MRG in xoy plane

tissue. At various frequencies, such as 3.6 GHz, 7.4 GHz, and 9.8 GHz, the antenna’s SAR value is 0.292/0.375/0.785 W/Kg, respectively.

The antenna’s SAR value is determined using a three-layer modeled human tissue measures  $90 \times 90 \times 33$  mm CST Microwave Studio where, particularly muscle, fat and skin tissues that are 2 mm, 6 mm, and 23 mm thick. The dielectric characteristics of the human tissue model at the frequencies of 3.6 GHz, 7.4 GHz and 9.8 GHz are shown in Tables 2, 3 and 4, respectively.

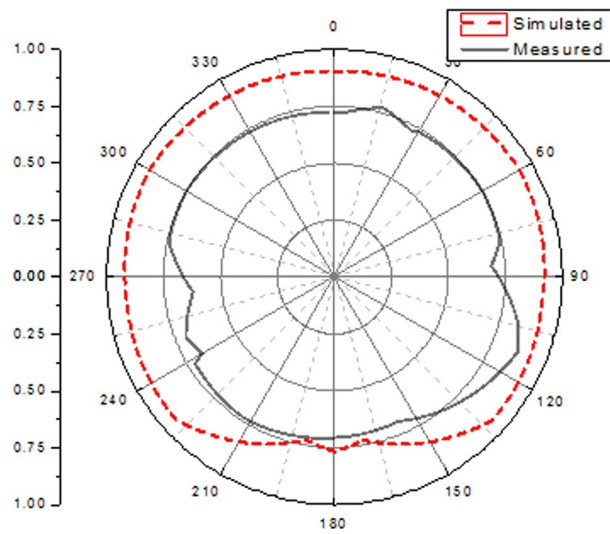


**Fig. 10** Fidelity factor variation

**Table 1** Comparison of proposed antenna with existing antenna

References	Operating frequency band (GHz)	Dimension (mm <sup>2</sup> )	Radiation pattern	Gain (dBi)
[6]	3.4–3.75 and 5.6–6	150 × 77	Directional	2–5
[7]	7.5–11.1	45 × 15	Omni	2.5
[8]	4.8–9.11	30 × 29	Omni	2–4
[9]	2.4	80 × 80	Directional	3
[10]	2.86–9.53	26 × 31	Omni	4
Proposed antenna	2.5–10.97	17.5 × 30	Omni	3–5

**Table 2** Dielectric characteristics of human tissue at 3.6 GHz

Layers	$\epsilon_r$	$\sigma$ (S/m)	Thickness (mm)
Muscle	53.67	0.36	23
Fat	5.36	0.17	6
Skin	40.4	0.47	2

**Table 3** Dielectric characteristics of human tissue at 7.4 GHz

Layers	$\epsilon_r$	$\sigma$ (S/m)	Thickness (mm)
Muscle	50.9	3.03	23
Fat	5.13	0.18	6
Skin	36.3	2.14	2

**Table 4** Dielectric characteristics of human tissue at 9.8 GHz

Layers	$\epsilon_r$	$\sigma$ (S/m)	Thickness (mm)
Muscle	42.86	4.96	23
Fat	4.60	0.29	6
Skin	31.28	3.69	2

#### 4 Conclusion

A UWB antenna with a unique shape of patch has been proposed for WBANs applications, and it is fabricated and tested on the human membrane. This proposed antenna has benefits of both conventional and printed antennas. The radiation performance is ideal for WBAN applications. The asymmetrical slotted patch with a diminished ground plane was introduced to broaden impedance bandwidth. The simulation results as well as measured results achieved 126 percent improvement in impedance bandwidth over the frequency ranges from 2.50 to 10.97 GHz. The wearable performance of the proposed UWB antenna has just a minor influence on human body. The obtained SAR value is 0.785 W/kg which is less than threshold Value. Behavior of the proposed UWB antenna in the time domain is evident in that it can transmit and receive pulse signals.

#### Abbreviations

UWB	Ultra Wide Band
WBANs	Wireless Body Area Networks
PCBs	Printed Circuit Boards
FCC	Federal Communications Commission
SAR	Specific Absorption Rate
IEC	International Electro-technical Commission

#### Author contributions

SJ performed simulation and analyzed the results. GM validated the results drafted the manuscript. All authors read and approved the final manuscript.

#### Funding

The authors have no funding. This work is fully self-supported.

#### Availability of data and materials

Data sharing not applicable to this article as no datasets were generated or analyzed during the current study.

#### Declarations

##### Competing interests

The authors declare that they have no competing interests.

Received: 21 March 2022 Accepted: 3 October 2022

Published online: 17 October 2022

#### References

1. B. Mohamadzade, R.B.V.B. Simorangkir, R.M. Hashmi, K.P. Esselle, A low profile, UWB circular patch antenna with monopole-like radiation characteristics, in *2020 International Workshop on Antenna Technology (iWAT)*, pp. 1–3. IEEE (2020)
2. FCC, Revision of Part 15 of the Commission's Rules Regarding UWB Transmission Systems, April 22, 2002
3. X. Begaud, *Ultra Wide Band Antennas* (John Wiley & Sons, Hoboken, NJ, 2013)
4. C.A. Balanis, *Modern Antenna Handbook* (Wiley, New York, 2008)
5. K.J. Li, C.Z. Du, G.Y. Jin, Z.L. Zhao, W.Q. Zheng, et al., A wideband CPW-fed monopole hexagon antenna for UWB applications, in *International Conference on Microwave and Millimeter Wave Technology (ICMMT)*, pp. 1–3 (2020)
6. N. OjaroudiParchin, H. JahanbakhshBasherlou, R.A. Abd-Alhameed, Design of multi-mode antenna array for use in next-generation mobile handsets. *Sensors* **20**(9), 2447 (2020)

7. N. Kushwaha, R. Kumar, An UWB fractal antenna with defected ground structure and swastika shape electromagnetic band gap. *Prog. Electromagn. Res B* **52**, 383–403 (2013)
8. B.S. Srikanth, S.B. Gurung, S. Manu, G.N. Gowthami, T. Ali, S. Pathan, A slotted UWB monopole antenna with truncated ground plane for breast cancer detection. *Alex. Eng. J.* **59**(5), 3767–3780 (2020)
9. S. Dhamodharan, G. Mohanbabu, Breast cancer detection using adaptable textile antenna design. *J. Med. Syst.* **43**, 177 (2019)
10. S. Dhamodharan, G. Mohanbabu, Design of compact UWB antenna for the detection of breast cancer tumor. *Int. J. Adv. Sci. Technol.* **29**(3), 5945–5956 (2020)
11. E. Guariglia, Harmonic Sierpinski gasket and applications. *Entropy* **20**, 714 (2018)
12. E. Guariglia, Entropy and fractal antennas. *Entropy* **18**(3), 84 (2016)
13. E. Guariglia, *Fractional-Wavelet Analysis of Positive Definite Distributions and Wavelets on  $D'(C)$*  (Springer, Berlin, 2016)
14. K.C. Hwang, A modified Sierpinski fractal antenna for multiband application. *IEEE Antennas Wirel. Propag. Lett.* **6**, 357–360 (2007)
15. R.C. Guido et al., Introduction to the discrete Shapelet transform and a new paradigm: joint time-frequency-shape analysis, in *IEEE International Symposium on Circuits and Systems (ISCAS)*, pp. 2893–2896 (2008)
16. M.V. Berry, Z.V. Lewis, J.F. Nye, On the Weierstrass–Mandelbrot fractal function. *Proc. R. Soc. Lond. A* **370**, 459–484 (1980)

### Publisher's Note

Springer Nature remains neutral with regard to jurisdictional claims in published maps and institutional affiliations.

Submit your manuscript to a SpringerOpen<sup>®</sup> journal and benefit from:

- Convenient online submission
- Rigorous peer review
- Open access: articles freely available online
- High visibility within the field
- Retaining the copyright to your article

---

Submit your next manuscript at ► [springeropen.com](https://www.springeropen.com)

---